

Calix[4]arene-Based Single-Molecule Magnets**

Georgios Karotsis, Simon J. Teat, Wolfgang Wernsdorfer, Stergios Piligkos, Scott J. Dalgarno,* and Euan K. Brechin*

Single-molecule magnets (SMMs)^[1] have been the subject of much interest in recent years because their molecular nature and inherent physical properties allow the crossover between classical and quantum physics to be observed.^[2] The macroscopic observation of quantum phenomena, such as tunneling between different spin states^[3] or quantum interference between tunnel paths,^[4] not only allows scientists to study quantum mechanical laws in great detail, but also provides model systems with which to investigate the possible implementation of spin-based solid state qubits^[5] and molecular spintronics.^[6] The isolation of small, simple SMMs is therefore an exciting prospect. To date, almost all SMMs have been made by the self-assembly of 3d metal ions in the presence of bridging or chelating organic ligands.^[7] However, very recently an exciting new class of SMMs based on 3d metal clusters (or single lanthanide ions) housed within polyoxometalates^[8] has appeared. These types of molecule, in which the SMM is completely encapsulated within (or shrouded by) a “protective” organic or inorganic sheath, have much potential for design and manipulation: for example, for the removal of unwanted dipolar interactions, the introduction of redox activity, or to simply aid functionalization for surface grafting.^[9]

Calix[4]arenes are cyclic, typically bowl-shaped polyphenols that have been used extensively in the formation of versatile self-assembled supramolecular structures.^[10]

Although many have been reported, *p*-*t*Bu-calix[4]arene and calix[4]arene (TBC4 and C4 respectively, Figure 1 a) are frequently encountered owing to their synthetic accessibility

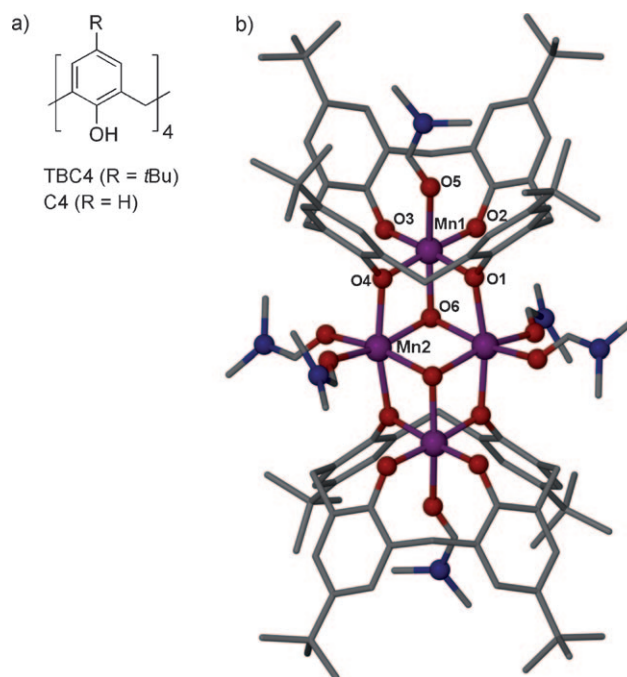


Figure 1. a) Structure of the calix[4]arenes used herein for SMM formation. b) Single-crystal X-ray structure of **1**. Mn purple, O red, N blue, C gray. Hydrogen atoms are omitted for clarity.

and the vast potential for alteration at either the upper or lower rim of the macrocyclic framework.^[11] Within the field of supramolecular chemistry, TBC4 is well-known for interesting polymorphic behavior and phase transformations within antiparallel bilayer arrays, whilst C4 often forms self-included trimers.^[12] The polyphenolic nature of calix[*n*]arenes (where *n* = 4–8) also suggests they should be excellent candidates as ligands for the isolation of molecular magnets, but to date their use in the isolation of paramagnetic cluster compounds is rather limited.^[13] Herein we present the first manganese cluster and the first SMM to be isolated using any methylene bridged calix[*n*]arene: a mixed-valence {Mn^{III}₂Mn^{II}₂} complex housed between either two TBC4 or two C4 moieties.

Reaction of MnBr₂ with TBC4 and NEt₃ in a solvent mixture of MeOH/DMF results in the formation of the complex [Mn^{III}₂Mn^{II}₂(OH)₂(TBC4)₂(dmf)₆] (**1**), which crystallizes as purple blocks. The cluster (Figure 1 b) comprises a planar diamond or butterfly-like {Mn^{III}₂Mn^{II}₂(OH)₂} core in which the wing-tip manganese ions (Mn1) are in the oxidation

[*] Dr. S. J. Dalgarno
School of Engineering and Physical Sciences, Heriot-Watt University
Riccarton, Edinburgh, EH14 4AS (UK)
Fax: (+44) 131-451-3180
E-mail: s.j.dalgarno@hw.ac.uk

G. Karotsis, Dr. E. K. Brechin
School of Chemistry, The University of Edinburgh
West Mains Road, Edinburgh, EH9 3JJ (UK)
Fax: (+44) 131-650-6453
E-mail: ebrechin@staffmail.ed.ac.uk

Dr. W. Wernsdorfer
Institut Néel, CNRS and Université J. Fourier
Grenoble Cedex 9 (France)

Dr. S. Piligkos
Department of Chemistry, University of Copenhagen
Universitetsparken 5, 2100 Copenhagen (Denmark)

Dr. S. J. Teat
Advanced Light Source, Berkeley Laboratory
1 Cyclotron Road, MS6R2100, Berkeley, CA 94720 (USA)

[**] The Advanced Light Source is supported by the Director, Office of Science, Office of Basic Energy Sciences, of the US Department of Energy under contract no. DE-AC02-05CH11231.

Supporting information for this article is available on the WWW under <http://dx.doi.org/10.1002/anie.200904094>.

state +3, and the body manganese ions (Mn2) are in the oxidation state +2. This is a common structural type in manganese SMM chemistry,^[14] but the oxidation state distribution in **1** is highly unusual, being “reversed” from the norm in which the body manganese ions are almost always +3. Indeed, such a reversed core has been seen only once before, in the cluster $[\text{Mn}^{\text{III}}_2\text{Mn}^{\text{II}}_2(\text{teaH})_2(\text{acac})_4(\text{MeOH})_2]^{2+}$ (**2**; teaH₃ = triethanolamine, Hacac = acetylacetonate) and its analogues.^[15] The Mn³⁺ ions are in distorted octahedral geometries, with the Jahn–Teller axes defined by O5(dmf)–Mn1–O6(OH). The four equatorial sites are occupied by the oxygen atoms (O1–O4) of the TBC4, two of which bridge in a μ_2 -fashion to the central Mn²⁺ ions (Mn1–O4–Mn2 103.5°; Mn1–O1–Mn2 105.4°). These units are connected to each other (Mn2–O6–Mn2' 94.7°) and to the Mn³⁺ ions (Mn1–O6–Mn2 100.4°; Mn1–O6–Mn2' 98.8°) by two μ_3 -bridging OH[–] ions, with the two remaining equatorial sites (completing the distorted octahedral geometry on Mn2) filled by terminal dmf ligands. There are no intermolecular hydrogen bonds between symmetry equivalents of **1**, with the closest interactions being between neighboring dmf ligands being circa 3.3 Å. The only intermolecular interaction with the core of **1** is from a disordered methanol molecule that hydrogen-bonds to O4.

Notably, the orientation of the *endo*-TBC4 dmf ligand in **1** is atypical, and is driven by coordination. To our surprise, we could not find a report on the solid-state structure of the DMF solvate of TBC4. Solvothermal recrystallization of TBC4 from DMF resulted in the formation of large colorless crystals that are in a tetragonal cell, which is common for solvates of TBC4.^[16] Structural analysis shows the expected bilayer arrangement in which the DMF molecules are oriented with methyl groups inserted into the calixarene cavity (Figure 2a and Supporting Information, Figure S1). For comparison, the extended structure of **1** (Figure 2b) shows a bilayer type arrangement that is skewed relative to that in TBC4·DMF. This is most likely attributable to the restriction on TBC4 orientation that is dictated by cluster formation in addition to the presence of the peripheral dmf ligands on Mn2 and Mn2' (Figure 1b). Furthermore, the almost completely encapsulated cavity-bound dmf ligand in **1** should have little effect over bilayer orientation relative to TBC4·DMF given that guest protrusion from the cavity is similar in both cases (Supporting Information, Figures S2 and S3, respectively). Although the extended structure in **1** does deviate from true planarity, the clusters are nevertheless arranged in bilayers that have an interlayer separation of about 19 Å (Figure 2b).

With respect to the magnetic properties of **1**, direct-current susceptibility measurements were carried out in the 300–5 K temperature range in an applied field of 0.1 T. The room-temperature $\chi_M T$ value of 15.5 cm³ K mol^{–1} is larger than the spin-only value expected for an uncoupled $[\text{Mn}^{\text{III}}_2\text{Mn}^{\text{II}}_2]$ unit of 14.75 cm³ K mol^{–1} (Figure 3a). The value then increases very slowly with decreasing temperature, reaching a maximum of circa 25 cm³ K mol^{–1} at 5 K. The behavior, which is similar to that reported for other $[\text{Mn}^{\text{III}}_2\text{Mn}^{\text{II}}_2]$ clusters, is suggestive of dominant but weak intramolecular ferromagnetic exchange.^[14] The experimental data can be satisfactorily fitted using the isotropic $2J$ model shown in the inset of Figure 3a,^[14b] affording the parameters

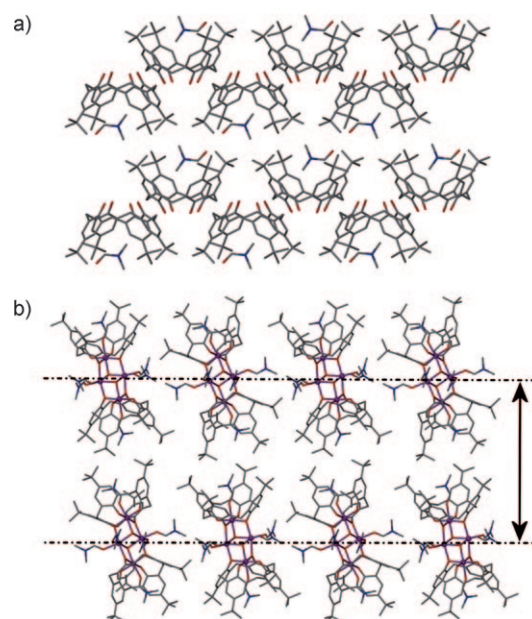


Figure 2. a) Extended structure of TBC4·DMF. b) Extended structure of **1** with the interplanar separation between layers of clusters (ca. 19 Å) indicated with an arrow. Hydrogen atoms omitted for clarity.

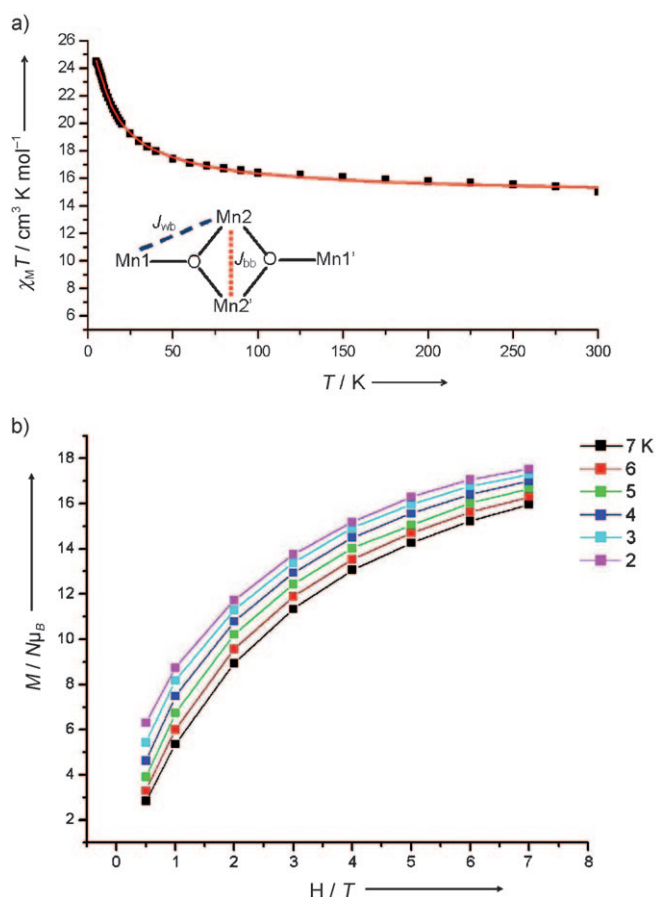


Figure 3. a) Plot of $\chi_M T$ versus T for **1**. The solid line is a fit of the experimental data using the cartoon scheme shown in the inset. b) Magnetization ($M/N\mu_B$) versus H data in the temperature range 2–7 K.

$J_{bb} = -2.43 \text{ cm}^{-1}$ and $J_{wb} = +1.84 \text{ cm}^{-1}$ for $g = 2.0$ (fixed). With these parameters, the spin ground state of the system is $S = 7$ (Supporting Information, Figure S4), with numerous excited states lying just above it, defining a quasi continuum of states. Interestingly, the magnitude of the exchange interactions closely resembles that observed for **2**, but in that case, distortions of the $\text{Mn}^{2+}\text{-O-Mn}^{2+}$ central core resulted in all the exchange interactions being very weakly antiferromagnetic.^[15] We also note that the exchange interactions are likely much smaller than the single ion zfs of the Mn^{III} ions (weak exchange limit). Thus, the low-lying multiplets cannot properly be described by the total spin quantum number S .

This picture is also reflected in the magnetization (M) versus field (H) data collected in the ranges 0.5–7.0 T and 2–7 K (Figure 3b), which shows M increasing only slowly with H , rather than quickly reaching saturation as would be expected for an isolated spin ground state. This result is indicative of the population of low-lying levels with smaller magnetic moment, which only become depopulated with the application of a large field, and so the system cannot be described within the giant spin approximation. Alternating current susceptibility studies carried out on crystalline samples of **1** in the 1.8–10.0 K range in a 3.5 G field oscillating at frequencies up to 1000 Hz (Supporting Information, Figure S5) display the tails of frequency-dependent out-of-phase (χ'') signals that are suggestive of SMM behavior, but no peaks. Hysteresis loop measurements carried out on single crystals using a micro-SQUID assembly with the field applied along the easy axis of magnetization^[17] show temperature- and sweep-rate-dependent hysteresis loops, thus confirming SMM behavior (Figure 4). The loops are indicative of a well-isolated SMM (that is, no intercluster interactions) with quantum steps, but one in which many excited states are clearly mixed with the ground state, which is in agreement with the powder data above. In addition to the contribution of excited states, factors such as crystal defects, nuclear spins, dipolar interactions, and/or disorder (if present) will also lead to the broadening of steps.

To demonstrate generality, replacing TBC4 with C4 in the reaction to form the SMM resulted in the formation of thin, weakly diffracting purple crystals. X-ray diffraction studies showed the crystals to be of poor quality, but afforded a

partial structure. Formation of the C4-based SMM core in **3**, which is analogous to **1**, was confirmed in the partial structure by observation of the main atomic positions (Figure 5). The extended structure shows that **3**, relative to **1**, assembles as a bilayer with a markedly shorter interlayer spacing of about 13.5 Å (Figure 5b). This reduced interlayer spacing is most

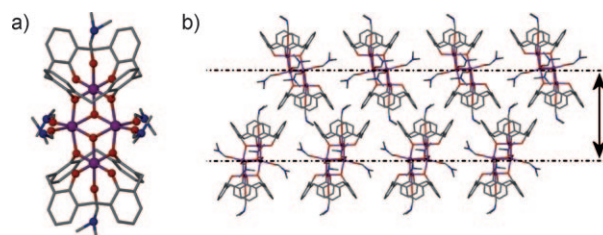


Figure 5. a) Partial single-crystal X-ray structure of **3**. b) The extended partial structure of **3** showing the interplanar separation between layers of SMMs (ca. 13.5 Å) indicated with an arrow. Hydrogen atoms omitted for clarity.

likely to be due to both removal of the *tert*-butyl groups from the upper rim and subsequent protrusion of the dmf methyl groups from the C4 cavity. As a result of cavity occupation, there appears to be no notable interactions between neighboring C4 moieties (Supporting Information, Figure S6). This clearly shows that substitution at the calixarene upper rim has a dramatic effect on assembly within resulting bilayers, and suggests that alteration of these groups may afford a degree of supramolecular control with this system.

In conclusion, we have presented the first manganese SMM cluster to be isolated using a methylene-bridged calix[*n*]arene. This SMM formation is general for calix[4]arenes, and given the vast range of methylene-bridged derivatives available, this motif presents a virtually unbounded range of SMMs that possess huge scope for materials design. The calix[4]arenes provide a protective skin both above and below the SMM layer, and alteration to the upper rim properties of the calixarene framework will provide control over bilayer packing, interlayer spacing, and three-dimensional order in general. Alteration of the guest in the calixarene cavity, and also the ligands at the peripheral manganese coordination sites, will provide further opportunities for controlling self-assembly and tuning of the magnetic properties of these new SMMs. These points will be the focus of future studies, as will be obtaining a more accurate structure of **2** and examining its magnetic properties.

Experimental Section

1: $\text{MnCl}_2 \cdot 4\text{H}_2\text{O}$ (0.1 g, 0.5 mmol) and TBC4 (0.1 g, 0.15 mmol) were dissolved in a mixture of DMF (10 mL) and MeOH (10 mL) and stirred for 1 hour. X-ray quality crystals were obtained in good yield (40%) after slow evaporation of the mother liquor. Elemental analysis (%) calculated for $\text{C}_{106}\text{H}_{146}\text{Mn}_4\text{N}_6\text{O}_{16}$: C 64.30, H 7.43, N 4.24; Found: C 64.02, H 7.54, N 4.21.

Crystal data for TBC4·DMF: $\text{C}_{47}\text{H}_{63}\text{N}_1\text{O}_5$, $M_r = 722.0$, colorless blocks, $0.50 \times 0.42 \times 0.38 \text{ mm}^3$, tetragonal, space group $P4/n$ (No. 85), $a = b = 12.6880(18)$, $c = 13.001(2)$ Å, $V = 2093.0(5)$ Å³, $Z = 2$, Bruker Nonius X8 Apex II diffractometer, MoK_α radiation, $\lambda = 0.71073$ Å,

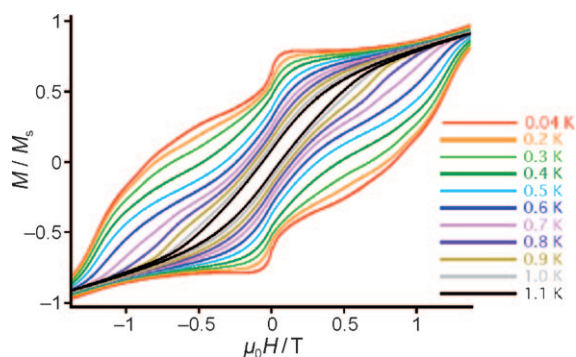


Figure 4. Hysteresis loops measured on single crystals of **1** at the indicated temperatures and a field sweep rate of 0.14 T s^{-1} . M is normalized to its magnetization value M_s at 1.4 T and 0.04 K.

$T=100(2)$ K, $2\theta_{\max}=49.8^\circ$; 7253 reflections collected, 1825 unique ($R_{\text{int}}=0.0613$). Final $\text{Goof}=1.134$, $RI=0.0652$, $wR2=0.1650$, R indices based on 1340 reflections with $I>2\sigma(I)$ (refinement on F^2). A number of restraints were applied owing to disorder in the DMF guest molecule and the *tert*-butyl groups of TBC4.

Crystal data for **1**: $\text{C}_{108}\text{H}_{154}\text{Mn}_4\text{N}_6\text{O}_{18}$, $M_r=2044.13$, purple blocks, $0.44\times0.38\times0.20\text{ mm}^3$, monoclinic, space group $P2_1/c$ (No. 14), $a=20.455(3)$, $b=11.2777(17)$, $c=24.513(4)\text{ \AA}$, $\beta=111.871(2)^\circ$, $V=5247.8(13)\text{ \AA}^3$, $Z=2$, Bruker Apex II CCD diffractometer, synchrotron radiation, $\lambda=0.77490\text{ \AA}$, $T=100(2)\text{ K}$, $2\theta_{\max}=50.4^\circ$, 42709 reflections collected, 7304 unique ($R_{\text{int}}=0.0868$). Final $\text{Goof}=1.018$, $RI=0.0551$, $wR2=0.1418$; R indices based on 5120 reflections with $I>2\sigma(I)$ (refinement on F^2).

Unit cell parameters for the partially solved structure of **3**: Monoclinic, space group $P2_1/c$ (No. 14), $a=12.6152(23)$, $b=12.5692(22)$, $c=28.1584(54)\text{ \AA}$, $\beta=105.859(3)^\circ$, Bruker Apex II CCD diffractometer, synchrotron radiation, $\lambda=0.77490\text{ \AA}$, $T=100(2)\text{ K}$. The low quality of the crystals precluded full structural characterization.

CCDC 741028 (TBC4-DMF) and CCDC 741029 (**1**) contains the supplementary crystallographic data for this paper. These data can be obtained free of charge from The Cambridge Crystallographic Data Centre via www.ccdc.cam.ac.uk/data_request/cif.

Received: July 23, 2009

Published online: September 25, 2009

Keywords: calixarenes · magnetic properties · manganese · self-assembly · supramolecular chemistry

- [1] G. Christou, D. Gatteschi, D. N. Hendrickson, R. Sessoli, *MRS Bull.* **2000**, 25, 66–71.
- [2] D. A. Garanin, X. M. Hidalgo, E. M. Chudnovsky, *Phys. Rev. B* **1998**, 57, 13639–13654.
- [3] a) J. R. Friedman, M. P. Sarachik, J. Tejada, R. Ziolo, *Phys. Rev. Lett.* **1996**, 76, 3830–3833; b) L. Thomas, F. Lioni, R. Ballou, D. Gatteschi, R. Sessoli, B. Barbara, *Nature* **1996**, 383, 145–147.
- [4] a) A. Garg, *Europhys. Lett.* **1993**, 22, 205; b) W. Wernsdorfer, R. Sessoli, *Science* **1999**, 284, 133–135.
- [5] a) M. N. Leuenberger, D. Loss, *Nature* **2001**, 410, 789–793; b) F. Troiani, A. Ghirri, M. Affronte, S. Carretta, P. Santini, G. Amoretti, S. Piligkos, G. A. Timco, R. E. P. Winpenny, *Phys. Rev. Lett.* **2005**, 94, 207208; c) A. Ardavan, O. Rival, J. J. L. Morton, S. J. Blundell, A. M. Tyryshkin, G. A. Timco, R. E. P. Winpenny, *Phys. Rev. Lett.* **2007**, 98, 057201.
- [6] L. Bogani, W. Wernsdorfer, *Nat. Mater.* **2008**, 7, 179–186.
- [7] G. Aromí, E. K. Brechin, *Struct. Bonding* **2006**, 122, 1–69.
- [8] a) C. Ritchie, A. Ferguson, H. Nojiri, H. N. Miras, Y.-F. Song, D.-L. Long, E. Burkholder, M. Murrie, P. Kögerler, E. K. Brechin, L. Cronin, *Angew. Chem.* **2008**, 120, 5691–5694; *Angew. Chem. Int. Ed.* **2008**, 47, 5609–5612; b) M. A. AlDamen, J. M. Clemente-Juan, E. Coronado, C. Martí-Castaldó, A. Gaita-Ariño, *J. Am. Chem. Soc.* **2008**, 130, 8874–8875; c) J.-D. Compain, P. Mialane, A. Dolbecq, I. Martyr Mbomekallé, J. Marrot, F. Sécheresse, E. Rivière, G. Rogez, W. Wernsdorfer, *Angew. Chem.* **2009**, 121, 3123–3127; *Angew. Chem. Int. Ed.* **2009**, 48, 3077–3081.
- [9] A. Giusti, Gaëlle Charron, S. Mazerat, J.-D. Compain, P. Mialane, A. Dolbecq, E. Rivière, W. Wernsdorfer, R. N. Biboum, B. Keita, L. Nadjo, A. Filoramo, J.-P. Bourgoin, T. Mallah, *Angew. Chem.* **2009**, 121, 5049–5052; *Angew. Chem. Int. Ed.* **2009**, 48, 4949–4952.
- [10] For some examples of versatile self-assembled calix[4]arene structures, see: L. R. MacGillivray, J. L. Atwood, *Nature* **1997**, 389, 469–472; O. Ugono, K. T. Holman, *Chem. Commun.* **2006**, 2144–2146; T. Gerkenmeier, W. Iwanek, C. Agena, R. Froehlich, S. Kotila, C. Nather, J. Mattay, *Eur. J. Org. Chem.* **1999**, 2257–2262; E. S. Barrett, T. J. Dale, J. Rebek, Jr., *J. Am. Chem. Soc.* **2007**, 129, 3818–3819; S. J. Dalgarno, S. A. Tucker, D. B. Basil, J. L. Atwood, *Science* **2005**, 309, 2037–2039; P. Jin, S. J. Dalgarno, C. Barnes, S. J. Teat, J. L. Atwood, *J. Am. Chem. Soc.* **2008**, 130, 17262–17263.
- [11] For examples of upper- and lower-rim calix[4]arene modification, see: C. D. Gutsche, *Calixarenes 2001*, Kluwer Academic Publishers, **2001**, chap. 1 and references therein; I. Thondorf, A. Shivanyuk, V. Böhmer, *Calixarenes 2001*, Kluwer Academic Publishers, **2001**, chap. 2 and references therein.
- [12] For a recent review on aspects of the supramolecular properties of TBC4 and C4, see: S. J. Dalgarno, P. K. Thallapally, L. J. Barbour, J. L. Atwood, *Chem. Soc. Rev.* **2007**, 36, 236–245.
- [13] a) C. Desroches, G. Pilet, S. A. Borshch, S. Parola, D. Luneau, *Inorg. Chem.* **2005**, 44, 9112–9120; b) C. Desroches, G. Pilet, P. A. Szilágyi, G. Molnár, S. A. Borshch, A. Bousseksou, S. Parola, D. Luneau, *Eur. J. Inorg. Chem.* **2006**, 357–365; c) C. Aronica, G. Chastanet, E. Zueva, S. A. Borshch, J. M. Clemente-Juan, D. Luneau, *J. Am. Chem. Soc.* **2008**, 130, 2365–2371.
- [14] a) E. K. Brechin, J. Yoo, M. Nakano, J. C. Huffman, D. N. Hendrickson, G. Christou, *Chem. Commun.* **1999**, 783–784; b) J. Yoo, E. K. Brechin, A. Yamaguchi, M. Nakano, J. C. Huffman, A. L. Maniero, L.-C. Brunel, K. Awaga, H. Ishimoto, G. Christou, D. N. Hendrickson, *Inorg. Chem.* **2000**, 39, 3615–3623.
- [15] L. M. Wittick, L. F. Jones, P. Jensen, B. Moubarak, L. Spiccia, K. J. Berry, K. S. Murray, *Dalton Trans.* **2006**, 1534–1543.
- [16] For examples, see: G. D. Andreotti, R. Ungaro, A. Pochini, *J. Chem. Soc. Chem. Commun.* **1979**, 1005–1007; E. B. Brouwer, G. D. Enright, J. A. Ripmeester, *J. Am. Chem. Soc.* **1997**, 119, 5404–5412; J. L. Atwood, L. J. Barbour, A. Jerga, B. L. Schottel, *Science* **2002**, 298, 1000–1002.
- [17] a) W. Wernsdorfer, *Adv. Chem. Phys.* **2001**, 118, 99–190; b) W. Wernsdorfer, *Supercond. Sci. Technol.* **2009**, 22, 064013.